

Published in final edited form as:

Nature. 2009 June 18; 459(7249): 1000–1004. doi:10.1038/nature08020.

CCR7 signalling as an essential regulator of CNS infiltration in T-cell leukaemia

Silvia Buonamici^{1,2}, Thomas Trimarchi^{1,2}, Maria Grazia Ruocco^{1,3}, Linsey Reavie^{1,2}, Severine Cathelin^{1,2}, Brenton G. Mar⁴, Apostolos Klinakis⁵, Yevgeniy Lukyanov¹, Jen-Chieh Tseng¹, Filiz Sen^{1,2}, Eric Gehrie⁶, Mengling Li⁷, Elizabeth Newcomb¹, Jiri Zavadil¹, Daniel Meruelo¹, Martin Lipp⁸, Sherif Ibrahim¹, Argiris Efstratiadis⁵, David Zagzag¹, Jonathan S. Bromberg⁶, Michael L. Dustin^{1,3}, and Iannis Aifantis^{1,2}

¹Department of Pathology and New York University Cancer Institute, New York 10016, USA

²Helen L. and Martin S. Kimmel Stem Cell Center, New York University School of Medicine, New York, New York 10016, USA

³Program in Molecular Pathogenesis, Helen L. and Martin S. Kimmel Center for Biology and Medicine of the Skirball Institute of Biomolecular Medicine, New York University School of Medicine, New York, New York 10016, USA

⁴Department of Pediatrics, Columbia University Medical Center, New York, New York 10032, USA

⁵Department of Genetics and Development, Columbia University Medical Center, New York, New York 10032, USA

⁶Department of Gene and Cell Medicine, and the Immunology Institute, Mount Sinai School of Medicine, New York, New York 10029, USA

⁷Division of Biostatistics, New York University Cancer Institute, New York, New York 10016, USA

⁸Department of Tumor Genetics and Immunogenetics, Max-Delbrück-Center for Molecular Medicine, 13092 Berlin, Germany

Abstract

T-cell acute lymphoblastic leukaemia (T-ALL) is a blood malignancy afflicting mainly children and adolescents¹. T-ALL patients present at diagnosis with increased white cell counts and hepatosplenomegaly, and are at an increased risk of central nervous system (CNS) relapse^{2,3}. For that reason, T-ALL patients usually receive cranial irradiation in addition to intensified intrathecal chemotherapy. The marked increase in survival is thought to be worth the considerable side-effects associated with this therapy. Such complications include secondary tumours, neurocognitive deficits, endocrine disorders and growth impairment³. Little is known about the mechanism of leukaemic cell infiltration of the CNS, despite its clinical importance⁴. Here we show, using T-ALL animal modelling and gene-expression profiling, that the chemokine receptor CCR7 (ref. 5) is the essential adhesion signal required for the targeting of leukaemic T-cells into

©2009 Macmillan Publishers Limited. All rights reserved

Correspondence and requests for materials should be addressed to I.A. (iannis.aifantis@nyumc.org).

Author Contributions S.B., B.G.M. and I.A. designed experiments, performed experiments and wrote the manuscript. M.L.D., M.Li and M.G.R. performed the *in vivo* two-photon microscopy experiments and analysis. D.M. and J.-C.T. performed the bioluminescent imaging experiments. A.K. and A.E. generated the EF1-Notch1-IC mice. J.Z. performed the microarray data mining. Y.L., E.N. and D.Z. performed in the CNS pathology analysis. M.Lipp and J.S.B. assisted with experimental design, provided reagents and advice. T.T., L.R., S.C. and E.G. performed experiments.

Supplementary Information is linked to the online version of the paper at www.nature.com/nature.

the CNS. *Ccr7* gene expression is controlled by the activity of the T-ALL oncogene Notch1 and is expressed in human tumours carrying Notch1-activating mutations. Silencing of either CCR7 or its chemokine ligand CCL19 (ref. 6) in an animal model of T-ALL specifically inhibits CNS infiltration. Furthermore, murine CNS-targeting by human T-ALL cells depends on their ability to express CCR7. These studies identify a single chemokine–receptor interaction as a CNS ‘entry’ signal, and open the way for future pharmacological targeting. Targeted inhibition of CNS involvement in T-ALL could potentially decrease the intensity of CNS-targeted therapy, thus reducing its associated short- and long-term complications.

Recent studies have shown that mutations of the developmental regulator Notch1 can be identified in most T-ALL patients⁷. It is estimated that activation of the Notch1 signalling pathway occurs in at least 80% of all T-ALL cases^{7–10}. To investigate the mechanisms of T-ALL CNS infiltration and derive information that could be useful for treatment, we have attempted to establish animal models involving expression of oncogenic Notch1 (intracellular Notch1 fragment, Notch1-IC). The first model entails the transplantation of wild-type haematopoietic progenitors carrying Notch1-IC introduced by retroviral transfer (WT^{Notch-IC})¹¹. The second model is on the basis of *Cre/loxP* recombination and involves Mx-Cre mice crossed with partners carrying dormant transgenic Notch1-IC, which was knocked-in into the ubiquitously expressed *Eef1a1* locus¹². The dormant Notch1-IC exerts oncogenic action after excision of a DNA segment blocking its expression, when Cre is expressed in haematopoietic progenitor cells by the IFN- α -inducible Mx1 promoter after polyinosinic:polycytidylic acid (poly(I:C)) injection. Both models developed T-ALL, presented atypical CD4⁺ CD8⁺ T cells in the peripheral blood as well as characteristic pathological features of T-ALL (Fig. 1 and Supplementary Figs 1 and 2). Immunohistochemical analysis demonstrated that in both models Notch1-IC–EGFP⁺ (enhanced green fluorescent protein) and CD3⁺ leukaemic cells efficiently infiltrated the leptomeningeal spaces of the brain (Fig. 1b, c and Supplementary Fig. 1). Further studies showed that the CNS infiltration was progressive, and was initially detected in mice in which leukaemic blasts were readily detected in their peripheral blood (Supplementary Fig. 3) and secondary lymphoid tissue (data not shown). We were thus able to show that oncogenic Notch1-IC expression was able to induce T-ALL and target the transformed cells to the CNS.

We used a genome-wide transcriptome approach to identify Notch1-induced adhesion regulators that could be essential for CNS infiltration. Uncommitted haematopoietic progenitors were infected with Notch1-IC–EGFP⁺ retroviruses and gene expression was recorded 48 h later¹¹. Detailed data mining demonstrated that a considerable fraction of Notch-controlled genes are potential regulators of cell adhesion, migration and metastasis (Fig. 2a and Supplementary Table 1). The expression of a specific gene, the chemokine receptor *Ccr7*, was significantly upregulated (Fig. 2a, b), and its expression remained constant after several days of culture (data not shown). CCR7 overexpression and function was also confirmed by real-time PCR, flow cytometry analysis and *in vitro* chemotaxis assays towards its known chemokine ligands CCL19 and CCL21 (Fig. 2b–d). CCR7 is an attractive candidate because it is a known regulator of lymphocyte migration⁶ and has been suggested to be important for the trafficking of lymphocytes participating in CNS immunosurveillance^{13,14}. CCR7 functions through its interactions with CCL19 and CCL21 (ref. 6), and the expression and function of all three have been shown to be involved in the directional metastasis of several types of solid tumours, including melanomas and breast cancers^{15,16}.

To correlate Notch1 activation and CCR7 expression further, we analysed T-ALL lines containing Notch1-activating mutations and primary T-ALL samples. Notably, surface

CCR7 was expressed in 80% (4 out of 5) of T-ALL lines and in 73% (8 out of 11) of peripheral blood from primary T-ALL samples (Supplementary Fig. 4). CCR7 expression in the studied lines was dependent on Notch1 activation, as the repression of Notch1 processing due to the addition of γ -secretase inhibitors (DBZ or compound E) led to significant downregulation of CCR7 messenger RNA and protein expression (Supplementary Fig. 5 and not shown). To obtain a preliminary estimate of the importance of CCR7 expression in CNS infiltration, we selected two human T-ALL lines (Supplementary Fig. 4a), one that expressed (CEM/CCR7⁺) and one that did not express (DND41/CCR7⁻) the chemokine receptor, and infected them using a luciferase-expressing lentivirus. To study disease induction and progression, we transplanted the cells into lymphoid *Rag2*^{-/-} *Il2rg*^{-/-} hosts. We were able to demonstrate that the transplantation of an identical number of leukaemia cells led to distinct survival patterns, as hosts that received CEM/CCR7⁺ cells succumbed to the disease earlier than those receiving the DND41/CCR7⁻ cells (Fig. 3a). Using live animal bioluminescent imaging, we were able to demonstrate a higher tumour load in mice that received the CEM/CCR7⁺ cell line (Fig. 3b). Most importantly, the brain and spinal cord of hosts transplanted with CEM/CCR7⁺ (but not with DND41/CCR7⁻) were infiltrated by T-ALL cells. Further histopathological analysis confirmed the localization of the infiltrating cells in leptomeningeal spaces (Fig. 3c, d).

As a next step, we addressed the sufficiency of CCR7 overexpression for the recruitment of leukaemic T cells in the CNS. We expressed mouse CCR7 (mCCR7) in the DND41/CCR7⁻ human T-ALL cell line using a bicistronic retroviral vector expressing CCR7 in conjunction with expression of the mCherry fluorochrome (Supplementary Fig. 6a). We verified that retroviral transduction induced mCherry and mCCR7 expression, and that mCherry⁺ DND41 (DND41/mCCR7⁺) cells acquired the ability to efficiently respond to both CCL19 and CCL21 ligands (Supplementary Fig. 6b). Infected cells and control (mCherry-only expressing counterparts) were injected into *Rag2*^{-/-} *Il2rg*^{-/-} hosts. All recipients developed T-ALL (Fig. 3a, b) and no CNS infiltration was detected in the mice transplanted with the control DND41/CCR7⁻ cells. On the other hand, we were able to demonstrate that CCR7 ectopic expression was sufficient to allow these cells to infiltrate both the brain and the spinal cord (Fig. 3c, d).

Although these results indicate that CCR7 expression is sufficient to recruit leukaemic T-cells into the CNS, they do not address whether CCR7 alone is necessary for this function. We infected haematopoietic progenitors from *Ccr7*^{-/-} (CCR7(KO))¹⁷ and *Ccr7*^{+/+} (wild-type) mice with Notch1-IC-expressing retroviruses (CCR7(KO)^{Notch1-IC} and WT^{Notch1-IC}), and infected EGFP⁺ cells were transplanted into wild-type hosts (WT/CCR7(KO)^{Notch1-IC} and WT/WT^{Notch1-IC}). All recipient mice developed T-cell leukaemia, characterized by the detection of atypical peripheral blood CD4⁺ CD8⁺ cells as early as 2 weeks after transplant. As before, histopathological analysis showed notable tissue infiltration in all recipients (Supplementary Figs 2, 7 and data not shown). Hosts receiving leukaemic CCR7(KO) cells survived significantly longer than the hosts that received leukaemic wild-type cells (Supplementary Fig. 8). Although both hosts had similar leukaemic infiltration of most tissues, histopathological analysis of the CNS demonstrated that leukaemic CCR7(KO) cells were not found in the brain at 5 weeks after bone marrow transplantation, but leukaemic wild-type cells were (Fig. 4a). This was also true even at later time points just before the hosts succumbed, at 9–11 weeks after transplant (data not shown), uncoupling the tumour load to CNS infiltration. These results indicate that CCR7 is necessary for this process, and that the elimination of a single chemokine receptor *in vivo* is able to abrogate CNS involvement in T-ALL. CCR7 function seems to be specific for Notch1-induced T-cell malignancy, because deletion of this chemokine in two models of B-cell ALL failed to suppress CNS infiltration (Supplementary Fig. 9).

We then sought to exclude the possibility that CCR7-deficient cells do not infiltrate the CNS because of a more general defect in their ability to migrate. As discussed before, CCR7(KO)^{Notch1-IC} cells infiltrate as well as leukaemic wild-type cells into several tissues. Also, the peripheral blood of hosts reconstituted with CCR7(KO)^{Notch1-IC} contained a similar (or even an increased) number of leukaemic blasts (Supplementary Figs 2 and 7). To attain a more dynamic view of the ability of the migratory properties of CCR7(KO)^{Notch1-IC} and WT^{Notch1-IC} leukaemic cells, we used two-photon imaging microscopy and traced EGFP⁺ cells within the lymph nodes of living leukaemic hosts. As illustrated in Supplementary Movies 1 and 2, we were unable to demonstrate any differences in the ability of these cells to migrate within the lymph nodes. When individual cells were traced, no statistically significant differences were found between the velocity, turning angle, arrest coefficient, confinement and random walk¹⁸ of CCR7(KO)^{Notch1-IC} and WT^{Notch1-IC} cells (Supplementary Fig. 10). These results underlined the specificity of CCR7 function in the targeting of T-ALL cells to the CNS.

Although these studies clearly demonstrate the importance of CCR7-mediated leukaemic cell recruitment to the CNS, they do not identify the ligand involved. It was previously shown that both chemokines are expressed in brain–blood barrier endothelium in an animal model of experimental autoimmune encephalomyelitis^{19,20}. Moreover, CCL21 expression was detected previously in the choroid plexus—a possible site of lymphocyte entry into the subarachnoid space²¹. Thus, we performed immunohistochemical analyses to compare CCL19 and CCL21 expression in brain sections of control and leukaemic mice. CCL21 expression was undetectable in either sample (data not shown). However, CCL19 was detectable mainly in brain venules in the vicinity of infiltrating lymphocytes (Fig. 4b–g). Using immunofluorescence costaining, we confirmed that CD31⁺ endothelial cells produced CCL19 (Fig. 4f, g). In addition, we purified brain CD31⁺ endothelial cells and show a significant (8–10-fold when compared to CD31[−] brain cells) induction of *Ccl19* message (Supplementary Fig. 11). Furthermore, endothelial cells from leukaemic animals expressed moderately higher (~twofold) levels of *Ccl19* (Supplementary Fig. 12) when compared to endothelial brain cells from recipients that received EGFP-only infected cells (did not show any CNS infiltration). To prove that this slight overexpression is not, by itself, sufficient to attract CCR7⁺ T cells in the CNS, we have transplanted wild-type CD4⁺ T cells into leukaemic recipients. Analysis of recipient brain sections 12–16 h after transplantation failed to show any non-Notch1-IC–EGFP T-cell accumulation (Supplementary Fig. 12).

To prove the essential role of CCL19 expression, we modified our transplantation protocol and used *plt* mice as hosts, which lack CCL19 expression owing to a naturally occurring mutation²². We transplanted these mice (or background- and age-matched controls) with Notch1-IC-expressing haematopoietic progenitors (*plt*/WT^{Notch1-IC}). In agreement with our previous transplantations, *plt* mice survived longer than their wild-type counterparts (Supplementary Fig. 8). As before, there was an identical T-ALL induction and disease manifestation between different hosts, suggesting that the *plt* mutation does not affect leukaemic cell infiltration in peripheral lymphoid tissues (Supplementary Figs 2 and 7). However, leukaemic cells were unable to infiltrate the brain of *plt* hosts, further strengthening our argument that CCR7–CCL19 interactions are essential for CNS infiltration in T-ALL (Fig. 4a, b).

Our data demonstrated that a single chemokine–receptor pair is both necessary and sufficient for T-cell ALL leukaemic cell targeting to the CNS. Although CCR7 expression seems to be an important signal targeting T-ALL cells in the CNS, other factors that are present in transformed leukaemic cells but not in wild-type T cells are needed for CNS infiltration. These factors could include extra adhesion regulators (that is, integrins and metalloprotease, see Fig. 2a) that could potentially interact with CCR7 function. We believe

that our studies open the way for the development of different therapeutic protocols, in which specific adhesion antagonists²³ can be used together with either current chemotherapy-based protocols or molecularly targeted approaches, for example, the use of antagonists of Notch signalling¹. Putative T-ALL CNS infiltration antagonists could include inhibitors of CCR7 expression and function, as well as drugs targeting specific migration regulators, which could be activated by CCR7 signalling.

METHODS

Animals

C57BL/6 and *Rag2*^{-/-} *Il2rg*^{-/-} mice were purchased from Jackson Laboratories and Taconic Farms. CCR7(KO) and *plt* mice have been described previously^{17,22}. All mice were kept in specific pathogen-free animal facilities at the NYU-SOM and Mount Sinai Medical School. All animal procedures were performed in accordance to the guidelines of the Institutional Animal Care and Use Committee of the NYU-SOM.

Recombinant DNA constructs and retrovirus production and infection

The Notch1-IC retroviral plasmid, its parent CMMP-based vector²⁷, the pMXs IRES-mCherry retroviral vector and the pWPI lentivirus (a gift from E. Hernando) were used. Viral supernatants were generated as described previously²⁸. Isolation, retroviral infection and reconstitution experiments were performed as previously described²⁷.

Antibodies and reagents

Mouse CD4-APC, CD8-PE-Cy7, CCR7-PE, B22 and CD31, and human CCR7-PE and CD3-APC primary antibodies were purchased from BD Bioscience. Human CD3 antibody was obtained by DAKO. Mouse CCL19 and CCL21 were procured from R&D. Mouse CD31 was from Pharmingen. Cytokines and chemokines were obtained from Peprotech. Secondary antibodies were purchased from Jackson Laboratories. Immunohistochemical analysis was performed using standard methods as described previously¹¹.

Chemotaxis assays

Chemotaxis assays were performed as previously described²⁹.

Quantitative RT-PCR

RNA was isolated using RNeasy Plus Mini Kit (Qiagen) columns and used to synthesize cDNA with the SuperScript First-Strand Kit (Invitrogen). Real-time PCR was performed using iQ SYBR Green Supermix and an iCycler (Bio-Rad). Relative expression was determined from cycle threshold (C_T) values, and normalized using β -actin as an internal control. All primer oligonucleotides are available on request.

Bioluminescent imaging

Imaging of luciferase-tagged leukaemic cells were performed as previously described²⁴.

Intravital microscopy

Two-photon imaging was performed as previously described²⁵. Individual cell tracing and data analysis was performed as previously described²⁶.

Microarray analysis

The accession numbers for the individual array comparisons are Gene Expression Omnibus (GEO) series GSE6396, samples GSM147443, GSM147464 and GSM147508. Sample

preparation and processing is detailed previously¹¹. Pathway analysis of the microarray mRNA profiling results was performed using the Gene Ontology and KEGG pathway mapping within the web-based tool Database for Annotation, Visualization and Integrated Discovery. The results of category/pathway enrichment were manually curated for focused contents based on gene number and associated *P* value, and are summarized in Supplementary Table 1.

Supplementary Material

Refer to Web version on PubMed Central for supplementary material.

Acknowledgments

We are grateful to G. Randolph, E. Kuan and T. Vilimas for technical help and discussions. We would like to thank P. Lopez and G. De La Cruz for cell sorting; D. Littman, W. Carroll, E. Raetz, S. Lira and S. Schwab for advice and illuminating discussions; C. Loomis and the Histology Facility for advice and troubleshooting tips. This work was supported by the National Institutes of Health (RO1CA105129, RO1CA133379, R56AI070310, P30CA016087 to I.A., RO1AI41428, RO1AI072039 to J.S.B.), the American Cancer Society (RSG0806801 to I.A.), the Dana Foundation, The Chemotherapy Foundation, the Alex's Lemonade Stand Foundation (to I.A.), the Lauri Strauss Leukemia Foundation (to F.S.), the G&P Foundation, NYU Molecular Oncology and Immunology training grant (to S.B.), American Society of Hematology (to S.B.), Juvenile Diabetes Research Foundation (JDRF11-2008-90 and 5-2008-236 to J.S.B.), the National Cancer Institute (1 P01 CA97403, Project 2 to A.E.) and a gift from the Berrie Foundation (to A.E.). A.K. was supported by a Fellowship from the Jane Coffin Childs Memorial Fund for Medical Research.

References

1. Grabher C, von Boehmer H, Look AT. Notch 1 activation in the molecular pathogenesis of T-cell acute lymphoblastic leukaemia. *Nature Rev Cancer*. 2006; 6:347–359. [PubMed: 16612405]
2. Aifantis I, Raetz E, Buonamici S. Molecular pathogenesis of T-cell leukaemia and lymphoma. *Nature Rev Immunol*. 2008; 8:380–390. [PubMed: 18421304]
3. Pui CH, Howard SC. Current management and challenges of malignant disease in the CNS in paediatric leukaemia. *Lancet Oncol*. 2008; 9:257–268. [PubMed: 18308251]
4. Pui CH, Evans WE. Treatment of acute lymphoblastic leukemia. *N Engl J Med*. 2006; 354:166–178. [PubMed: 16407512]
5. Cyster JG. Chemokines, sphingosine-1-phosphate, and cell migration in secondary lymphoid organs. *Annu Rev Immunol*. 2005; 23:127–159. [PubMed: 15771568]
6. Forster R, Davalos-Miszlitz AC, Rot A. CCR7 and its ligands: balancing immunity and tolerance. *Nature Rev Immunol*. 2008; 8:362–371. [PubMed: 18379575]
7. Weng AP, et al. Activating mutations of *NOTCH1* in human T cell acute lymphoblastic leukemia. *Science*. 2004; 306:269–271. [PubMed: 15472075]
8. Thompson BJ, et al. The SCFFBW7 ubiquitin ligase complex as a tumor suppressor in T cell leukemia. *J Exp Med*. 2007; 204:1825–1835. [PubMed: 17646408]
9. Palomero T, et al. Mutational loss of PTEN induces resistance to NOTCH1 inhibition in T-cell leukemia. *Nature Med*. 2007; 13:1203–1210. [PubMed: 17873882]
10. O'Neil J, et al. *FBW7* mutations in leukemic cells mediate NOTCH pathway activation and resistance to γ -secretase inhibitors. *J Exp Med*. 2007; 204:1813–1824. [PubMed: 17646409]
11. Vilimas T, et al. Targeting the NF- κ B signaling pathway in Notch1-induced T-cell leukemia. *Nature Med*. 2007; 13:70–77. [PubMed: 17173050]
12. Klinakis A, et al. Igf1r as a therapeutic target in a mouse model of basal-like breast cancer. *Proc Natl Acad Sci USA*. 2009; 106:2359–2364. [PubMed: 19174523]
13. Charo IF, Ransohoff RM. The many roles of chemokines and chemokine receptors in inflammation. *N Engl J Med*. 2006; 354:610–621. [PubMed: 16467548]

14. Cardona AE, Li M, Liu L, Savarin C, Ransohoff RM. Chemokines in and out of the central nervous system: much more than chemotaxis and inflammation. *J Leukoc Biol.* 2008; 84:587–594. [PubMed: 18467654]
15. Muller A, et al. Involvement of chemokine receptors in breast cancer metastasis. *Nature.* 2001; 410:50–56. [PubMed: 11242036]
16. Shields JD, et al. Autologous chemotaxis as a mechanism of tumor cell homing to lymphatics via interstitial flow and autocrine CCR7 signaling. *Cancer Cell.* 2007; 11:526–538. [PubMed: 17560334]
17. Forster R, et al. CCR7 coordinates the primary immune response by establishing functional microenvironments in secondary lymphoid organs. *Cell.* 1999; 99:23–33. [PubMed: 10520991]
18. Mempel TR, Scimone ML, Mora JR, von Andrian UH. *In vivo* imaging of leukocyte trafficking in blood vessels and tissues. *Curr Opin Immunol.* 2004; 16:406–417. [PubMed: 15245733]
19. Kivisakk P, et al. Human cerebrospinal fluid central memory CD4⁺ T cells: evidence for trafficking through choroid plexus and meninges via P-selectin. *Proc Natl Acad Sci USA.* 2003; 100:8389–8394. [PubMed: 12829791]
20. Giunti D, et al. Phenotypic and functional analysis of T cells homing into the CSF of subjects with inflammatory diseases of the CNS. *J Leukoc Biol.* 2003; 73:584–590. [PubMed: 12714572]
21. Kivisakk P, et al. Expression of CCR7 in multiple sclerosis: implications for CNS immunity. *Ann Neurol.* 2004; 55:627–638. [PubMed: 15122702]
22. Gunn MD, et al. Mice lacking expression of secondary lymphoid organ chemokine have defects in lymphocyte homing and dendritic cell localization. *J Exp Med.* 1999; 189:451–460. [PubMed: 9927507]
23. Ransohoff RM. Natalizumab for multiple sclerosis. *N Engl J Med.* 2007; 356:2622–2629. [PubMed: 17582072]
24. Tseng JC, et al. Tumor-specific *in vivo* transfection with HSV-1 thymidine kinase gene using a Sindbis viral vector as a basis for prodrug ganciclovir activation and PET. *J Nucl Med.* 2006; 47:1136–1143. [PubMed: 16818948]
25. Shakhar G, et al. Stable T cell-dendritic cell interactions precede the development of both tolerance and immunity *in vivo*. *Nature Immunol.* 2005; 6:707–714. [PubMed: 15924144]
26. Mempel TR, Henrickson SE, Von Andrian UH. T-cell priming by dendritic cells in lymph nodes occurs in three distinct phases. *Nature.* 2004; 427:154–159. [PubMed: 14712275]
27. Sicinska E, et al. Requirement for cyclin D3 in lymphocyte development and T cell leukemias. *Cancer Cell.* 2003; 4:451–461. [PubMed: 14706337]
28. Ory DS, Neugeboren BA, Mulligan RC. A stable human-derived packaging cell line for production of high titer retrovirus/vesicular stomatitis virus G pseudotypes. *Proc Natl Acad Sci USA.* 1996; 93:11400–11406. [PubMed: 8876147]
29. Scimone ML, Aifantis I, Apostolou I, von Boehmer H, von Andrian UH. A multistep adhesion cascade for lymphoid progenitor cell homing to the thymus. *Proc Natl Acad Sci USA.* 2006; 103:7006–7011. [PubMed: 16641096]

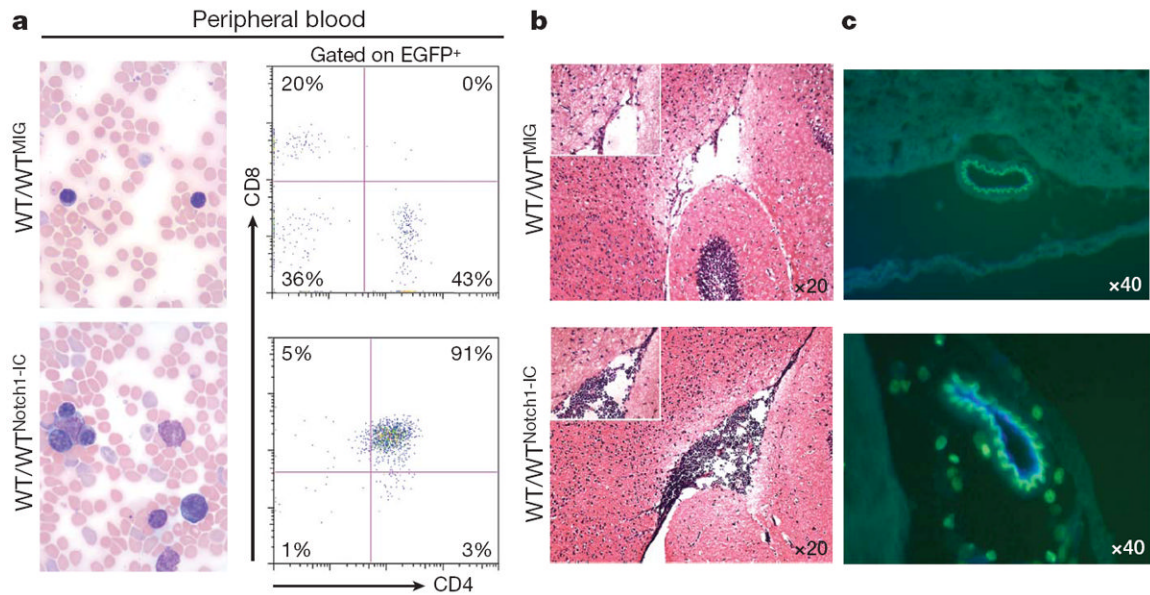


Figure 1. Notch1 activation induces T-ALL and targets leukaemic cells into the CNS
a, Induction of T-ALL in a transplantation model (WT/WT^{Notch1-IC}). Peripheral blood smears (left), and fluorescence-activated cell sorting (FACS, right) analysis using CD4 and CD8 antibodies are shown. ‘WT^{MIG}’ denotes wild-type bone marrow infected with a control MIG retrovirus. **b**, Notch1-IC⁺ EGFP⁺ cells in the brain meningeal spaces of transplanted mice. **c**, Infiltrating lymphocytes surrounding a brain vessel in leukaemic (bottom panel) but not in healthy (control, top panel) recipients. Co-staining with CD31 antibodies (blue) indicates endothelial cells within the infiltrating lymphocytes.

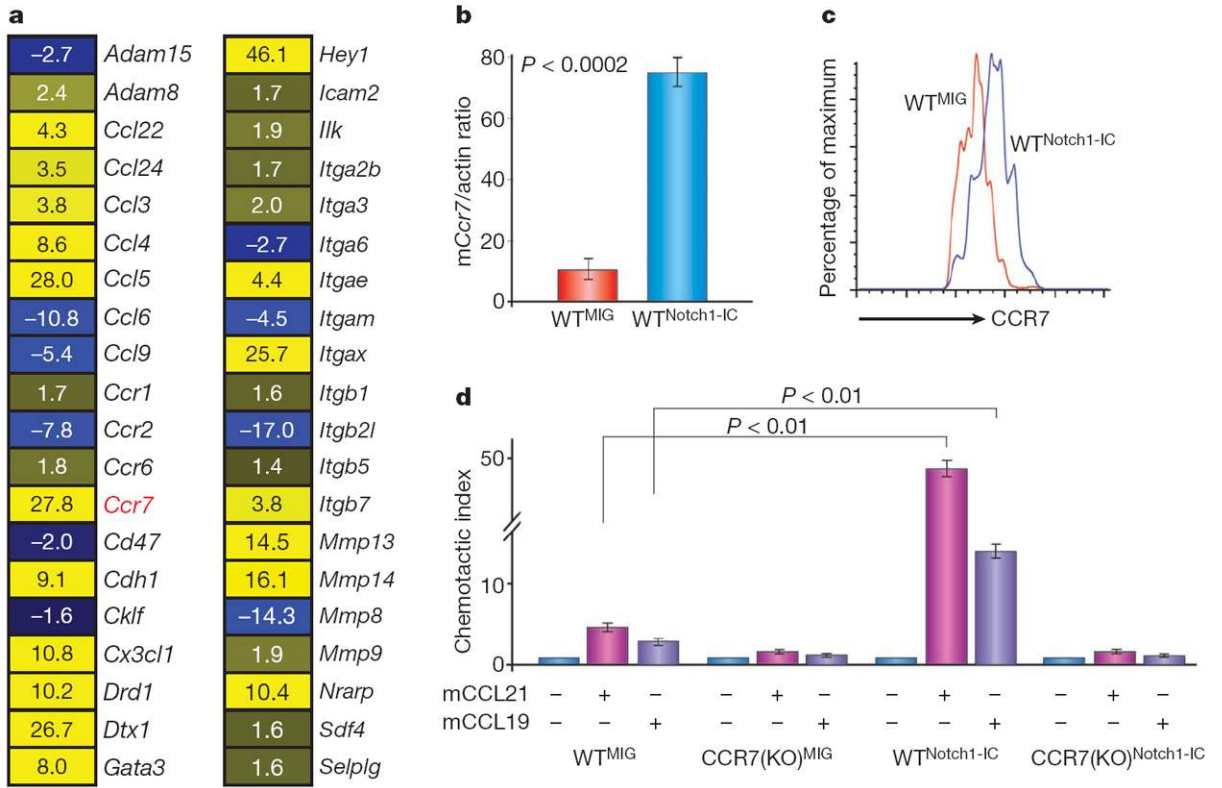


Figure 2. CCR7 expression and response to CCL19/CCL21 is induced by Notch1 activation
a, Heat diagram of selected adhesion/migration regulators that are controlled by Notch1-IC. A few classical Notch targets (*Dtx1*, *Gata3*, *Hey1* and *Nrarp*) are also included. For all genes, $P < 0.001$. Yellow and blue denote increased and decreased mRNA abundance, respectively. **b**, **c**, Real-time PCR (**b**) and FACS (**c**) analysis showing the induction of CCR7 gene and protein expression in haematopoietic progenitors in response to Notch1-IC expression; $n = 4$. **d**, Notch1-IC expression induces the chemotaxis of wild-type ($WT^{Notch1-IC}$), but not $CCR7(KO)^{Notch1-IC}$ progenitors towards both CCL19 and CCL21; $n = 3$. Error bars define s.d. for all experiments.

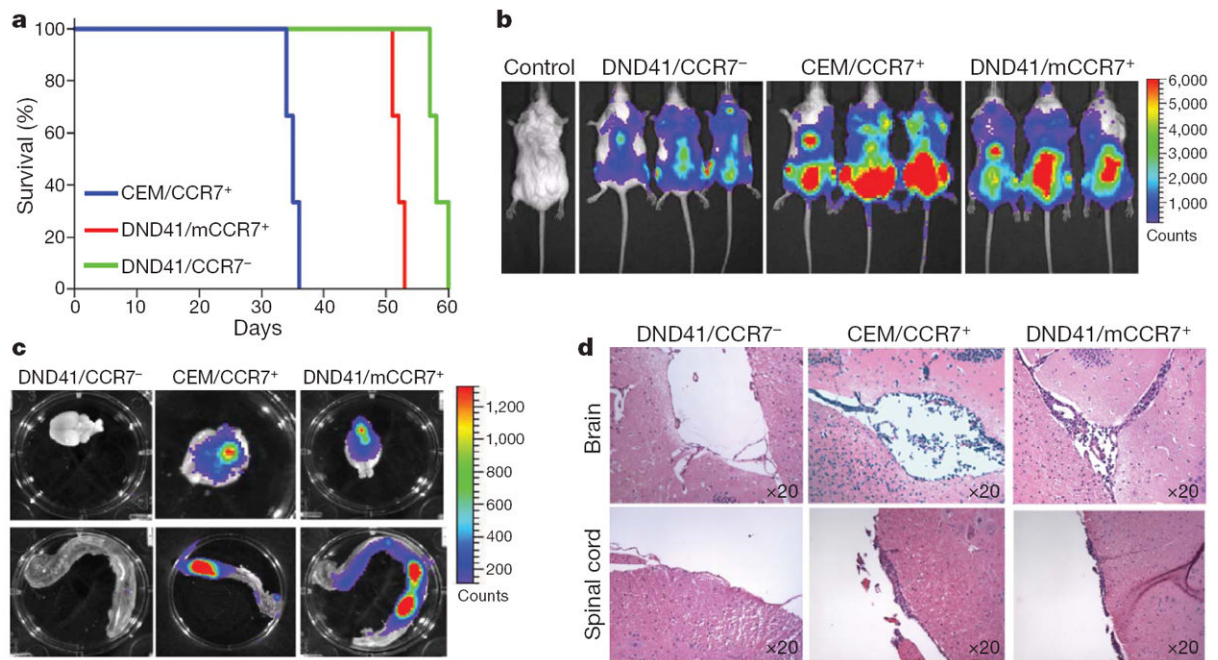


Figure 3. CCR7 expression is sufficient for CNS infiltration of human T-ALL cells

a, Kaplan–Meyer analysis of recipients that received identical numbers of CEM, DND41 or DND41/mCCR7⁺ cells; $n=5$.

b, Bioluminescent imaging of mice 2 weeks after transplantation with the indicated cell lines. **c–d**, Infiltration of T-ALL cells into the CNS of recipient mice as shown using bioluminescence and histochemistry.

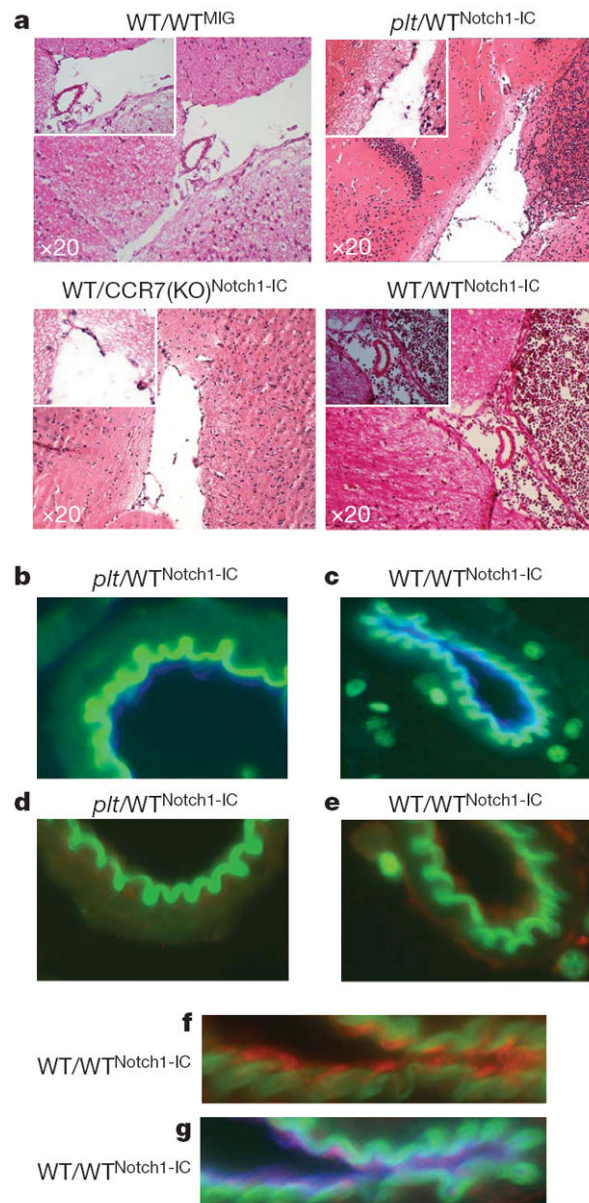


Figure 4. CCR7–CCL19 interactions are essential for CNS infiltration in an animal model of T-ALL

a, Leukaemic cells in the brain meningeal spaces of the indicated transplanted recipients. A positive control (WT/WT^{Notch1-IC}) is also included. **b–g**, Immunofluorescent staining of brain sections: magnification of a brain microvessel in *plt*/WT^{Notch1-IC} (**b**) and WT/WT^{Notch1-IC} (**c**) mice. Endothelial, CD31⁺ cells are shown in blue. **d–g**, CCL19 (red) expression in WT/WT^{Notch1-IC} (**e**, **f**, **g**) but not *plt*/WT^{Notch1-IC} (**d**) microvessels. **f**, **g**, Magnification of a WT/WT^{Notch1-IC} microvessel and costaining with CCL19 (red) and CD31 (blue).